

STATUS AND PERSPECTIVES FOR THE SWISS FREE-ELECTRON LASER (SwissFEL)

T. Schietinger* on behalf of the SwissFEL team
Paul Scherrer Institut, Villigen, Switzerland

Abstract

We summarize the status of SwissFEL, the X-ray free-electron laser at the Paul Scherrer Institute. Apart from some key operational performance figures the contribution covers the state of the experimental stations, the evolution of user demand and gives a brief overview of the use of advanced operation modes beyond SASE at our facility. Furthermore we report on progress of our seeding upgrade program on the soft X-ray line. Lastly we mention our long-term upgrade plans for a third undulator beamline in the tender and hard X-ray regime.

INTRODUCTION

SwissFEL is a free-electron laser (FEL) facility at the Paul Scherrer Institute in Switzerland featuring two beamlines, Aramis for the hard X-ray regime (1.8–12.4 keV) and Athos covering the soft X-ray spectrum (0.26–1.9 keV) [1]. The accelerator consists of an S-band photoinjector gun followed by an S-band booster radiofrequency (rf) linac, which accelerates electron bunches to an energy of 300 MeV. Main acceleration to the final beam energy of up to 6.2 GeV (Aramis) is accomplished through a series of C-band rf linacs.

A schematic view of the SwissFEL facility is given in Fig. 1. The electron gun generates two bunches, separated by 28 ns, at a repetition rate of 100 Hz. The first bunch goes straight to the Aramis undulator line, while the second bunch is extracted at a beam energy of 3.17 GeV into a dogleg beamline leading to the Athos undulator. A short tuning linac in the Athos branch allows for energy adjustments in the range ± 250 MeV. The electron bunches are compressed longitudinally in two magnetic chicanes (BC1 and BC2). In the Aramis branch they may be further compressed in an energy collimator chicane before the undulator, in Athos in the dogleg and in additional chicanes present in that beamline. The Aramis undulator line consists of 13 planar in-vacuum undulator modules of 4 m length each with 15 mm period. Athos features 2×8 highly flexible APPLE-X type undulator modules, which are 2 m long and have 38 mm period. The Athos undulator modules are interspersed with small magnetic delaying chicanes. Between the two undulator halves there is a larger chicane used for tuning the delay (up to 500 fs) between two-color pulses generated individually in the two undulator halves. All undulators have adjustable deflecting parameters K through variable gaps (up to a maximum value of 1.8 in Aramis, 3.8 in Athos). For more details we refer to the “first-lasing” publications for Aramis [2] and Athos [3] and references therein.

Several deflecting rf cavities at different locations along the accelerator are used for measurements of the bunch profile or longitudinal phase space. An S-band deflecting cavity after BC1 performs such measurements with a temporal resolution of about 10 fs, whereas two C-band deflecting cavities at the end of linac-3 provide subfemtosecond resolution [4]. In 2022, a set of two X-band rf deflecting cavities for postundulator measurements in the Athos line was installed and commissioned, marking the completion of the SwissFEL baseline design. The cavities are based on the PolariX design, which arose from a collaboration between DESY, CERN and PSI [5]. The system gives time-resolved information on the lasing process with subfemtosecond resolution [6] and is indispensable for the clean setup of the many advanced operation modes available in Athos. Longitudinal phase space measurements of similar quality can also be obtained by streaking the beam passively with the wakefields from metallic corrugated structures [7].

SwissFEL ENDSTATIONS

Each of the SwissFEL undulator lines is designed to deliver FEL pulses to one out of three endstations associated with that line. Pairs of offset mirrors are set to ensure transport of the X-rays to the desired endstations. The endstations are named after Swiss mountain passes: Alvra, Bernina and Cristallina at the Aramis line, Maloja, Furka and Diavolezza at the Athos line.

At the Aramis line, Alvra and Bernina have been in operation since the beginning of FEL operation, with pilot runs in 2018 followed by the start of regular user operation in 2019. Alvra focuses on ultrafast dynamics of photochemical and photobiological systems while Bernina primarily measures ultrafast phenomena in condensed matter systems. The third endstation, Cristallina, designed for quantum science and structural biology, is currently in its pilot phase and will switch to user operation at the beginning of 2024.

The Athos undulator line was completed in the course of 2020. The first endstation, Maloja, started its pilot run at the end of that year and moved on to regular user operation in the beginning of 2022. Its focus lies on atomic, molecular and nonlinear X-ray physics and chemical dynamics. The second endstation, Furka, addresses ultrafast dynamics in quantum matter. Its pilot phase began in early 2023 and is planned to last for about one year. Finally, a third endstation, to be called Diavolezza and dealing with attosecond and nonlinear X-ray science, is in a conceptual phase and expected to become operational in a few years.

* thomas.schietinger@psi.ch

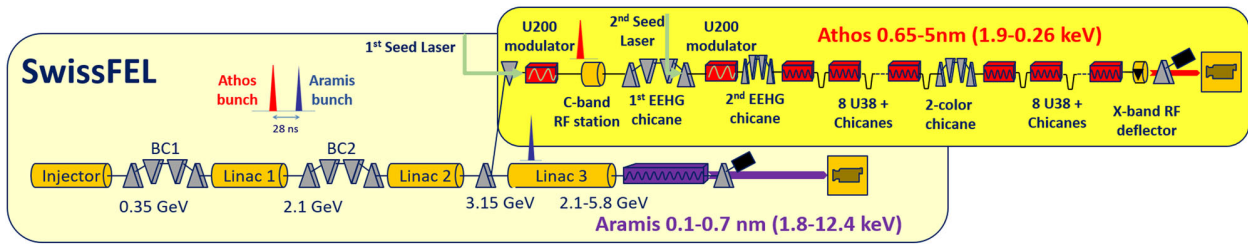


Figure 1: Schematic of SwissFEL accelerator layout (from Ref. [3]).

OPERATIONAL PERFORMANCE

For regular SASE operation, SwissFEL has achieved a level of performance that is close to the theoretically expected limit for a machine of its type. In Aramis, both electron energy and undulator K values are adjusted to reach a given photon energy. Whenever possible, the undulator is set to the maximum K value of about 1.75 to benefit from the strongest FEL coupling (with suitably tapered K values towards the end of the undulator line to compensate for electron energy loss). Only at the highest photon energies (above 9 keV), the K values are lowered to match the resonance condition with a 6-GeV electron beam. At the highest K and electron energy, a photon pulse energy of about 1.5 mJ can be extracted from the FEL at a resulting photon energy around 9 keV. This value drops to about 1.0 mJ at 2.5 keV photon energy (operating at a lower electron energy) or 0.9 mJ at 12.4 keV (operating at lower K values). In many cases, users ask for shorter pulses, which can only be achieved by either restricting the number of electrons that lase or reducing the overall number of electrons in the beam, with corresponding reductions in pulse energy.

In Athos the adjustment of the photon energy mainly hinges on the variation of the K values, since the tuning of the electron energy is limited to the ± 250 MeV provided by the one C-band rf station installed between the switchyard and the undulator line. Accordingly, the photon pulse energy drops from a maximum of around 5 mJ at 0.5 keV down to below 1.2 mJ at 1.2 keV. (The FEL has not yet been optimized over the entire photon energy range.)

The achieved pulse energies are largely reproducible from one experiment to the next. The overall beam availability of the facility primarily depends on hardware failures. It is rather high for an FEL, reaching 95.8% for Aramis and 96.1% for Athos in 2022 during user operation.

USER DEMAND

Figure 2 shows the overall numbers of submitted and accepted experiment proposals at SwissFEL for the years 2018 through 2022 (top), as well as the corresponding numbers for experiment days (bottom). One experiment day equals three eight-hour shifts. A first period of euphoria is followed by a leaner period due to the Covid pandemic. In particular the low numbers of 2021 can be explained by the need to catch up the backlog of experiments granted for 2020 but

postponed during the height of the pandemic. Most recently, user numbers have been on the rise again, not least because the two new endstations Cristallina and Maloja became available to the general user community.

It is interesting to see which photon energies generate the most interest among users. Figure 3 shows the distribution of shifts in 2022 and 2023 (up to August) as a function of photon energy delivered by the FEL for Aramis and Athos, respectively.

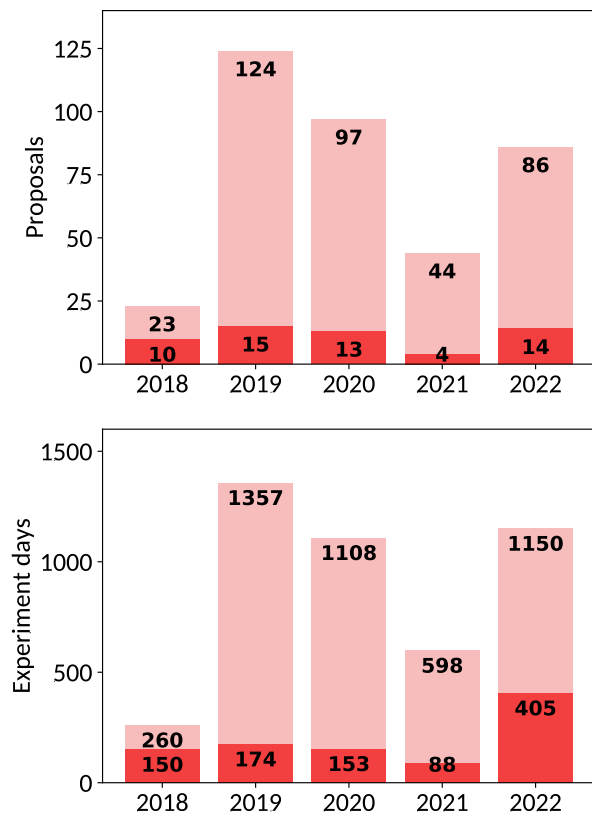


Figure 2: Evolution of the number of submitted (light red) and accepted (dark red) experiment proposals at SwissFEL (top). Corresponding evolution of the number of requested and granted experiment days (bottom, same color code). Each experiment day corresponds to three shifts of eight hours each.

The SwissFEL measurement periods lead to a steady stream of publications in a wide range of fields in science and technology. A recent highlight was the elucidation of the light-triggered structural changes of the molecule retinal inside the light-receptor protein rhodopsin with the help of data gathered at SwissFEL [8].

ADVANCED FEL OPERATION MODES – ARAMIS

At the Aramis beamline, by far the most often demanded FEL operation mode beyond SASE is a short-pulse mode in which photon pulses are shortened by applying a tilt to the electron beam, which limits the length over which the beam is aligned with the undulator axis such that it can sustain the FEL process [9]. In this way, photon pulses down to 2–3 fs duration (rms) can be generated routinely, albeit with a corresponding reduction in pulse energy. The beam tilt is typically realized by utilizing the wakefields from a set of flat parallel plates with microstructured surfaces (the same devices can be used to remove a residual energy chirp in the beam).

The Aramis line provides a large-bandwidth operation mode, which is based on a strong energy chirp in the electron

beam, further enhanced by exploiting the strong wakefields arising from the C-band driving linac [10]. By leaking out dispersion into the undulator line it is possible to split up the wavelengths spatially, i.e., add a spatial chirp to the photon beam (large bandwidth with spatial chirp) [11]. Both types of large-bandwidth operation modes have been demonstrated and exploited in user experiments, with further experiments of this kind in the pipeline.

Extremely short FEL pulses, so-called “attosecond pulses” with duration well below one femtosecond can be generated by nonlinear compression of a low-charge electron beam in three stages [12]. For this operation mode the energy collimator chicane just in front of the undulator line is used as a third compression stage. The resulting FEL pulses exhibit very few individual radiation spikes, with a large fraction (about 40%) of fully coherent single-spike pulses. The operation mode was recently exploited for coherent small-angle X-ray scattering (cSAXS) measurements on quantum magnets by the Cristallina endstation and is expected to become a standard operation mode for this endstation.

ADVANCED FEL OPERATION MODES – ATHOS

We refer to Ref. [13] for an overview of the numerous advanced operation modes possible with Athos. A number of these modes have been made available to users, others are still in a commissioning phase, and some modes have not been attempted yet, either because of a lack of user demand or because further improvements to the machine are necessary before they can be tackled.

Early on, the shortening of the saturation length thanks to the optical-klystron effect could be demonstrated with the entire Athos undulator line [14]. This is of particular importance for modes where only a part of the undulator is available to reach saturation at a given wavelength, such as in the two-color mode.

Similar to Aramis, also in Athos pulses shorter than those resulting from the normal SASE process are in high demand. Again this can be achieved with a beam tilt, but in contrast to Aramis here the beam tilt is controlled by the dispersion present in the dogleg of the Athos extraction line acting on the energy-chirped beam. (In principle also in Athos the beam tilt can be generated through wakefields, but this method was found to result in higher beam losses.)

The generation of FEL pulses with variable polarization represents one of the Athos beamline’s main attractions [3]. Several user experiments have already exploited the straightforward switching between circular and linear polarizations afforded by Athos.

The two-color mode in Athos makes use of a split-undulator configuration, in which each half of the undulator generates one wavelength (color). Both the standard approach, in which the full electron bunch lases, and the fresh-slice approach, in which each color is generated with a different part (slice) of the bunch, have been demonstrated successfully [15]. The latter approach, which has the ad-

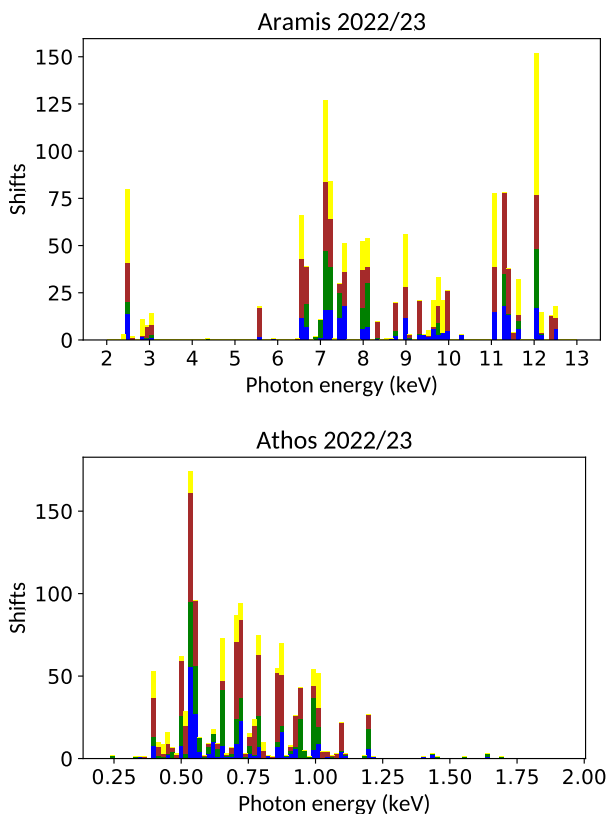


Figure 3: Number of shifts in 2022 and 2023 (until August) as a function of the set photon energy for the Aramis (top) and Athos (bottom) lines. Yellow: user experiment shifts, brown: user beamline development shifts, green: machine development shifts, blue: machine setup shifts.

Content from this work may be used under the terms of the CC-BY-4.0 licence (© 2023). Any distribution of this work must maintain attribution to the author(s), title of the work, publisher, and DOI

vantage of delivering short pulses with the option of zero or even negative time delays between the colors, has already been applied in several user experiments.

Steady progress has been made in the very challenging high-power short-pulse mode (also known as multistage amplification mode), where the radiation pulse from a short slice of the electron bunch is further amplified, in several stages, by unspoiled electrons from new slices along the bunch, thereby exploiting the superradiant regime of the FEL. Currently about a millijoule of pulse energy can be achieved within a pulse length of a few femtoseconds [16]. The operation mode was recently applied in a test experiment at the Maloja endstation.

Last but not least we mention the recent successful demonstration of sub-femtosecond (“attosecond”) pulses also in the Athos line [17]. As in Aramis, a low-charge bunch is subjected to strong nonlinear compression in three stages, but in this case the dogleg of the Athos switchyard serves as the third compression stage.

ATHOS SEEDING UPGRADE

The provision for seeding the soft X-ray line has been included in the design of building complex and associated infrastructure from the very beginning of the SwissFEL project, but was not part of the baseline design for financial reasons. The upgrade of the Athos line to enable laser-based seeding of the FEL process was then realized during the initial user operation phase, in two stages. In a first step a seed laser, with central wavelengths of 790 and 390 nm, and a 200 mm period magnetic modulator were installed in the framework of the so-called “HERO” project (named after the funding ERC project “Hidden and Entangled Resonating Order” [18]). This part of the upgrade was already sufficient to demonstrate the generation of attosecond pulse trains by energy-modulating the electron beam through overlap with the seed laser and converting the energy modulation into a density modulation in a chicane following the ESASE scheme [19]. An alternative method making use of a strong undulator taper [20] was also applied with success. The electron longitudinal phase space after energy modulation, measured with the X-band rf deflector and shown in Fig. 4, clearly exhibits the periodicity expected from the wavelength of the seed laser. In a next step, mode locking between the attosecond pulses by applying delays to the electron beam that match the laser wavelength was attempted, but no clean verification was possible at this point, given our lack of phase sensitive diagnostics.

The second stage of the upgrade comprises a second seed laser with another incoupling modulator (also 200 mm period), and a larger magnetic chicane, all necessary to put into practice echo-enabled harmonic generation (EEHG) [21]. As of this writing, all the components have been installed and tested individually. First attempts to implement and verify EEHG are planned very soon.

OUTLOOK

Midterm Improvements

SwissFEL is still in its early stages and is constantly being improved on various fronts. Here we mention two areas of further development.

A number of FEL operation modes are difficult to set up because of the inhomogeneous longitudinal electron beam profile coming out of the photoinjector. In particular head and tail of the bunch, where the charge density is lower and the energy chirp is less linear, are subject to overcompression, leading to two distinct peaks (“horns”) in the current profile. These parts of the beam feature significantly different beam properties giving rise to issues associated with beam transport, diagnostics and reduced lasing performance.

The only viable solution to this problem consists in collimating away both head and tail of the bunch (as is done at LCLS). The dispersive sections in the bunch compression chicanes are ideal locations to perform such collimation. Indeed it was confirmed that collimation in the first bunch compressor essentially fixes the problem, but the associated beam loss would not allow operation at 100 Hz. A radiation-shielding enclosure of the chicane was installed recently, but needs further iteration to meet our stringent radiation safety requirements.

A second challenge to be addressed in the near future concerns the stabilization of the EEHG mode in order to turn this mode from an experimental demonstration into a work horse for regular user experiments. This will require both improvements to the seed laser systems as well as a feedback loop keeping constant the overlap between laser and electron beam, based on suitable instrumentation monitoring the difference in arrival time. The previously mentioned cleaning of the longitudinal electron current profile is also an important prerequisite for the stable operation of EEHG.

In the longer term we are considering moving the first bunch compressor further upstream in order to reduce the

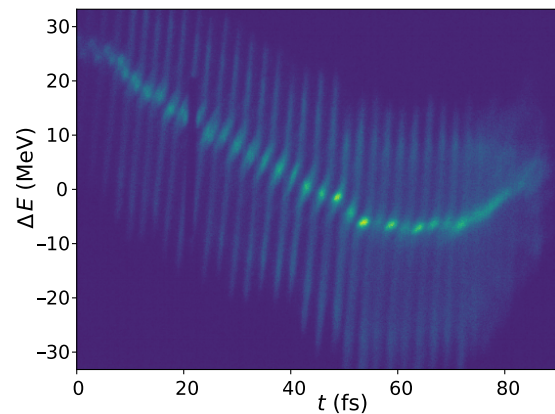


Figure 4: Electron longitudinal phase space (energy versus time) after energy modulation by a seed laser with 790 nm wavelength, as observed with the X-band rf deflector.

effects of microbunching and, in particular, intrabeam scattering on the energy spread.

Porthos Upgrade

In the longer run it is planned to expand the SwissFEL capabilities by adding a third beamline, which, in good Musketeer tradition, will go by the name of Porthos. The existing building and associated infrastructure already provide for a third beamline running in parallel to the Aramis beamline, including a beamdump. Preliminary work on the extraction line has already started in the framework of the PSI-CERN collaboration for building and testing a prototype of a positron source for the FCC-ee project [22]. Space for the experiments, however, is still missing, and a new experiment hall would have to be built for Porthos.

The science case for Porthos is still in development. A first iteration of the deliberations within the community was documented in the 2021 photon science roadmap [23] compiled by the Swiss photon community. More recent considerations suggest a photon energy range between 1 and 10 keV for Porthos, with an undulator line providing similar or even more flexibility than the existing Athos line, thus including polarization control and intra-undulator chicanes to delay the electron beam with respect to the emitted radiation.

The timescale for the implementation of Porthos is still uncertain, as PSI is strongly focused on its current flagship project, SLS-2.0, and a major upgrade of the proton facility to be realized afterwards.

CONCLUSION

After five years of user operation, SwissFEL has reached a stable level of performance, responding to the needs of a growing user community. By exploring new FEL modes, SwissFEL has established itself as one of the main drivers of FEL science, in particular in the soft X-ray regime with its extremely flexible Athos beamline. The extension of Athos to a laser-seeded FEL will make this beamline even more attractive for users. In the long term, a third beamline, probably covering the photon energy range between 1 and 10 keV and offering flexibility similar to Athos in that energy range, will further enhance the SwissFEL portfolio.

ACKNOWLEDGMENTS

We acknowledge the many contributions of all the PSI support groups involved in the operation and further development of the SwissFEL facility.

REFERENCES

- [1] C. J. Milne *et al.*, “SwissFEL: the Swiss X-ray free electron laser”, *Appl. Sci.*, vol. 7, p. 720, 2017. doi:10.3390/app7070720
- [2] E. Prat *et al.*, “A compact and cost-effective hard X-ray free-electron laser driven by a high-brightness and low-energy electron beam”, *Nat. Photonics*, vol. 14, p. 748, 2020. doi:10.1038/s41566-020-00712-8

- [3] E. Prat *et al.*, “An X-ray free-electron laser with a highly configurable undulator and integrated chicanes for tailored pulse properties”, *Nat. Commun.*, vol. 14, p. 5069, 2023. doi:10.1038/s41467-023-40759-z
- [4] E. Prat, A. Malyzhenkov, and P. Craievich, “Sub-femtosecond time-resolved measurements of electron bunches with a C-band radio-frequency deflector in x-ray free-electron lasers”, *Rev. Sci. Instrum.*, vol. 94, p. 043103, 2023. doi:10.1063/5.0144876
- [5] P. Craievich *et al.*, “Novel X-band transverse deflection structure with variable polarization”, *Phys. Rev. Accel. Beams*, vol. 23, p. 112001, 2020. doi:10.1103/PhysRevAccelBeams.23.112001
- [6] P. Craievich *et al.*, “Post-undulator beam measurements with PolariX TDS in SwissFEL”, *Proc. of SPIE*, vol. 12581, p. 1258106, 2023. doi:10.1117/12.2665447
- [7] P. Dijkstal *et al.*, “Self-synchronized and cost-effective time-resolved measurements at x-ray free-electron lasers with femtosecond resolution”, *Phys. Rev. Res.*, vol. 4, p. 013017, 2022. doi:10.1103/PhysRevResearch.4.013017
- [8] T. Gruhl *et al.*, “Ultrafast structural changes direct the first molecular events of vision”, *Nature*, vol. 615, p. 939, 2023. doi:10.1038/s41586-023-05863-6
- [9] P. Dijkstal, E. Prat, and S. Reiche, “Short FEL pulses with tunable duration from transversely tilted beams at SwissFEL”, in *Proc. FEL'22*, Trieste, Italy, Aug. 2022, pp. 121–125. doi:10.18429/JACoW-FEL2022-MOP51
- [10] E. Prat *et al.*, “Demonstration of large bandwidth hard X-Ray free-electron laser pulses at SwissFEL”, *Phys. Rev. Lett.*, vol. 124, p. 074801, 2020. doi:10.1103/PhysRevLett.124.074801
- [11] S. Reiche *et al.*, “Frequency and spatially chirped free-electron laser pulses”, *Phys. Rev. Res.*, vol. 5, p. L022009, 2023. doi:10.1103/PhysRevResearch.5.L022009
- [12] A. Malyzhenkov *et al.*, “Single- and two-color attosecond hard x-ray free-electron laser pulses with nonlinear compression”, *Phys. Rev. Res.*, 2, p. 042018(R), 2020. doi:10.1103/PhysRevResearch.2.042018
- [13] R. Abela *et al.*, “The SwissFEL soft X-ray free-electron laser beamline: Athos”, *J. Synchrotron Radiat.*, vol. 26, p. 1073, 2019. doi:10.1107/S1600577519003928
- [14] E. Prat *et al.*, “Demonstration of a compact x-ray free-electron laser using the optical klystron effect”, *Appl. Phys. Lett.*, vol. 119, p. 151102, 2021. doi:10.1063/5.0064934
- [15] E. Prat *et al.*, “Widely tunable two-color x-ray free-electron laser pulses”, *Phys. Rev. Res.*, vol. 4, p. L022025, 2022. doi:10.1103/PhysRevResearch.4.L022025
- [16] G. Wang, E. Prat, S. Reiche, and K. Schnorr, “Progress on fresh-slice multi-stage amplification at SwissFEL”, presented at the 67th ICFA Advanced Beam Dynamics Workshop (FLS'23), Lucerne, Switzerland, Aug.-Sep. 2023, paper TH2A3, this conference.
- [17] E. Prat *et al.*, “Coherent sub-femtosecond soft X-ray free-electron laser pulses with nonlinear compression”, to be published.
- [18] G. Aepli, A. V. Balatsky, H. M. Rønnow, and N. A. Spaldin, “Hidden, entangled and resonating order”, *Nat. Rev. Mater.*, vol. 5, p. 477, 2020. doi:10.1038/s41578-020-0207-z

- [19] A. A. Zholents, “Method of an enhanced self-amplified spontaneous emission for x-ray free electron lasers”, *Phys. Rev. Spec. Top. Accel. Beams*, vol. 8, p. 040701, 2005. doi:10.1103/PhysRevSTAB.8.040701
- [20] E. L. Saldin, E. A. Schneidmiller, and M. V. Yurkov, “Self-amplified spontaneous emission FEL with energy-chirped electron beam and its application for generation of attosecond x-ray pulses”, *Phys. Rev. Spec. Top. Accel. Beams*, vol. 9, 050702, 2006. doi:10.1103/PhysRevSTAB.9.050702
- [21] G. Stupakov, “Using the beam-echo effect for generation of short-wavelength radiation”, *Phys. Rev. Lett.*, vol. 102, p. 074801, 2009. doi:10.1103/PhysRevLett.102.074801
- [22] N. Vallis *et al.*, “The PSI Positron Production Project”, in *Proc. LINAC’22*, Liverpool, UK, Aug.-Sep. 2022, pp. 577–580. doi:10.18429/JACoW-LINAC2022-TUPORI16
- [23] R. Abela, E. Abreu, A. Cavalieri, M. van Daalen, T. Feurer, and U. Staub, “Photon science roadmap for research infrastructures 2025–2028 by the Swiss photon community”, *Swiss Academies Reports*, vol. 16, no. 5, 2021. doi:10.5281/zenodo.4588917